(Article begins on next page)

Journal of Engineering for Gas Turbines and Power

Copy of e-mail Notification

Journal of Engineering for Gas Turbines and Power Published by ASME

Dear Author,
Congratulations on having your paper accepted for publication in the ASME Journal Program.
Your page proof is available from the ASME Proof site here:
http://cps.kwglobal.com/MIS/AuthorProofLogin.aspx?pwd=6b155150753e&CA=AS

Login: your e-mail address
Password: 6b155150753e

Please keep this email in case you need to refer back to it in the future.
Responsibility of detecting errors rests with the author. Please review the page proofs carefully and:
1. Answer any queries on the “Author Query Form”
2. Proofread any tables and equations carefully
3. Check to see that any special characters have translated correctly
4. Publication will not proceed until a response is received. If there are no corrections, a response is still required.

RETURNING CORRECTIONS:
Corrections must be returned using the ASME Proof Download & Corrections Submission Site (link above). You will be able to upload:
1. Annotated PDF
2. Text entry of corrections, with line numbers, in the text box provided
3. Additional files, if necessary.

SPECIAL NOTES:
Your Login and Password are valid for a limited time. Please reply within 48 hours.

Corrections not returned through the above website will be subject to publication delays.
This e-proof is to be used only for the purpose of returning corrections to the publisher. Please note, the figures in this proof are low resolution, the final paper will publish with all figures as 300 dpi.If you have any questions, please contact: asme.cenveo@cenveo.com, and include your article no. (GTP-18-1725) in the subject line. This email should not be used to return corrections.

Approval of these proofs re-confirms the copyright agreement provision that all necessary rights from third parties for any copyrighted material (including without limitation any diagrams, photographs, figures or text) contained in the paper has been obtained in writing and that appropriate credit has been included.

Sincerely,
Mary O'Brien, Journal Production Manager

STATEMENT OF EDITORIAL POLICY AND PRACTICE

The Technical Committee on Publications and Communications (TCPC) of ASME aims to maintain a high degree of technical, literary, and typographical excellence in its publications. Primary consideration in conducting the publications is therefore given to the interests of the reader and to safeguarding the prestige of the Society.

To this end the TCPC confidently expects that sponsor groups will subject every paper recommended by them for publication to careful and critical review for the purpose of eliminating and correcting errors and suggesting ways in which the paper may be improved as to clarity and conciseness of expression, accuracy of statement, and omission of unnecessary and irrelevant material. The primary responsibility for the technical quality of the papers rests with the sponsor groups.

In approving a paper for publication, however, the TCPC reserves the right to submit it for further review to competent critics of its own choosing if it feels that this additional precaution is desirable. The TCPC also reserves the right to request revision or condensation of a paper by the author or by the staff for approval by the author. It reserves the right, and charges the editorial staff, to eliminate or modify statements in the paper that appear to be not in good taste and hence likely to offend readers (such as obvious advertising of commercial ventures and products, comments on the intentions, character, or acts of persons and organizations that may be construed as offensive or libelous), and to suggest to authors rephrasing of sentences where this will be in the interest of clarity. Such rephrasing is kept to a minimum.

Inasmuch as specific criteria for the judging of individual cases cannot, in the opinion of the TCPC, be set up in any but the most general rules, the TCPC relies upon the editorial staff to exercise its judgment in making changes in manuscripts, in rearranging and condensing papers, and in making suggestions to authors. The TCPC realizes that the opinions of author and editor may sometimes differ, and hence it is an invariable practice that no paper is published until it has been passed on by the author. For this purpose page proofs of the edited paper are sent to the author prior to publication in a journal. Changes in content and form made in the proofs by authors are followed by the editor except in cases in which the Society's standard spelling and abbreviation forms are affected.

If important differences of opinion arise between author and editor, the points at issue are discussed in correspondence or interview, and if a solution satisfactory to both author and editor is not reached, the matter is laid before the TCPC for adjustment.

Technical Committee on Publications and Communications (TCPC)
Reviewed: 05/2012

AUTHOR QUERY FORM

ASME SETTING THE STANDARD	Journal: J. Eng. Gas Turbines Power Article Number: GTP-18-1725	Please provide your responses and any corrections by annotating this PDF and uploading it to ASME's eProof website as detailed in the Welcome email.

Dear Author,

Below are the queries associated with your article; please answer all of these queries before sending the proof back to Cenveo. Production and publication of your paper will continue after you return corrections or respond that there are no additional corrections.

Location in article	Query / Remark: click on the Q link to navigate to the appropriate spot in the proof. There, insert your comments as a PDF annotation.
AQ1	Reminder – the ASME Copyright Agreement that was signed by all authors includes the following: "You have the right to enter into this Copyright Form and to make the assignment of rights to ASME. If the Paper contains excerpts from other copyrighted material (including without limitation any diagrams, photographs, figures or text), you have acquired in writing all necessary rights from third parties to include those materials in the Paper, and have provided appropriate credit for that third-party material in footnotes or in a bibliography." As required, ASME may contact the authors to obtain a copy of the written permission.
AQ2	Any content obtained from the web and included in the paper may require written permission and appropriate credit if it is copyrighted content. If copyright status cannot be determined, this content should not be included in the paper.
AQ3	Please note the figures in this proof are low resolution, the final paper will publish with all figures as 300 dpi.
AQ4	Please provide department details and zipcode (postal code) for all the affiliations.
AQ5	In the sentence beginning "The first part consists…" please specify which section or subsection does the next subsection refers to here.
AQ6	In the sentence beginning "This allowed both surge…" please specify which section or subsection does the next subsection refers to here.
AQ7	Please define FFT at the first occurrence.
AQ8	Please provide conference date for Refs. 6, 8, and 9.
AQ9	Please provide DOI or website to access article for Ref(s). 7.

Thank you for your assistance.

AQ1
AQ2
AQ3
AQ4

Stall and Surge in Wet Compression: Test Rig Development and Experimental Results

Enrico Munari
■,
University of Ferrara,
Ferrara ■, Italy

Gianluca D'Elia
■,
University of Ferrara,
Ferrara ■, Italy

Mirko Morini
■,
University of Parma,
Parma ■, Italy

Michele Pinelli
■,
University of Ferrara,
Ferrara ■, Italy

Pier Ruggero Spina
■,
University of Ferrara,
Ferrara ■, Italy

Wet compression is a strategy adopted to increase the power output of gas turbines, with respect to dry conditions, usually also incrementing the operating range of the compressor. However, stall and surge are two aerodynamic instabilities which depend on many factors, and they are expected to occur even in wet compression at low flow rates. Despite the many studies carried out in the last 80 years, literature does not offer many works concerning these instability phenomena in wet compression. In this paper, an experimental analysis of stall and surge in wet compression conditions is carried out on an axial-centrifugal compressor installed in an existing test rig at the Engineering Department of the University of Ferrara. The intake duct was implemented with a water injection system (WIS) which allows the uniform mixing of air and water before the compressor inlet. The control and data acquisition system of the test bench was updated with new hardware and software to obtain faster data sampling. Transient and steady-state tests were carried out to make a comparison with the experimental results in dry conditions. The analysis was carried out using traditional thermodynamic sensors, by means of both classic post-processing techniques and cyclostationary analysis. The aim is to (i) evaluate the influence of wet compression on the stable performance of the compressor, (ii) qualitatively identify the characteristics of stall and surge in wet compression, and (iii) demonstrate the reliability of cyclostationary analysis in wet compression conditions for stall and surge analysis. [DOI: 10.1115/1.4042474]

Introduction

Currently, wet compression and inlet fogging represent approaches which are becoming more popular for the enhancement of turbomachinery performance [1–3].

The most important advantage of these methodologies is the increase in the power output of gas turbines, due to the reduction in the compressor inlet temperature, which is crucial for increasing the mass flow rate, due to evaporative cooling, and thus the energy produced by the machine operation (this advantage is also due to the lower compressor work required) [4–7].

Another important aspect to be considered is the reduction in pollutant emissions of gas turbines due to the decrease in the inlet and combustor temperature [8], which nowadays is becoming a relevant factor in industry. Obviously, the injection of water leads to greater benefits in hot seasons and in hot environments. In those circumstances, this approach can help to fulfill seasonal peaks of energy demands [9] but also sudden increases in electric demand [10].

Together with the known paybacks, inlet fogging and wet compression are accompanied by strong drawbacks, especially in the long term [11]. In fact, although many gas turbines use water injection (with droplets or fogged water) as "normal" operating conditions, this technique should not be employed for long periods but only for short periods of time. If this does not occur, the risk is blade erosion in the first stages of the compressor due to the continuous impact of water droplets (sometimes their formation can occur with inlet fogging also due to the malfunctioning of atomizers). However, there are still few available data in literature for the correct estimation of undesirable long-term consequences and their correlation with blade materials and coatings.

Another debated aspect is the reduction in the surge margin caused by wet compression technology [11,12]: this phenomenon is undoubtedly caused by erosion (see above) over the long-term period [6] but seems to be accentuated by the reduction in temperature along the stages, which is also the reason for the reduction in the flow coefficient and increase in the pressure ratio at the last compressor stages [13,14]. The stability limit and the behavior during instability with water injection are thus a relevant topic. Based on literature, some authors believe that the compressor curve shape has a significant impact on the limit value of the amount of water that can be injected in order to avoid surge [13]. Obviously, this is also related to the change in aerodynamics of the compressor, and thus the velocity triangles, with wet compression, or with inlet fogging.

Unfortunately, as mentioned previously, due to the fairly recent development of wet compression and inlet fogging, the issue of compressor instability conditions is not comprehensively understood and univocally interpreted. In fact, Day et al. [15] who studied the unstable behavior of an axial flow compressor with water ingestion, observed premature stall, which occurred in most of the tests. Similarly, Roumeliotis and Mathioudakis [16] reported a reduction in the stall margin and surge line due to water injection. These works are in contrast with what was found by Minghong and Qun [17] and Qun and Minghong [18] who presented data showing the stabilizing effect of wet compression on both rotating stall and surge. Their idea is supported by Gröner and Bakken [19] who analyzed the stability limit of a centrifugal compressor reporting a delay of instability onset thanks to the presence of liquid.

It appears clear that the contrasting results readily available suggest that the unstable behavior of compressors with wet compression technology still needs to be investigated further, mainly because it may lead to the need for new evaluations and implementations in antisurge and control systems.

In particular, with the exception of the references cited previously and the work of Ferrara and Bakken [20], not many other data are available in literature regarding the stall and surge phenomena with water injection. In this context, this paper aims to

Manuscript received December 1, 2018; final manuscript received December 31, 2018; published online xx xx, xxxx. Assoc. Editor: Tim Allison.

improve the knowledge of stall and surge phenomena mechanisms with wet compression, by presenting significant experimental data obtained from a test rig installed at the University of Ferrara.

This facility replaces the old one—a preliminary test rig presented in Ref. [21]—and is dedicated to the study of unstable behavior of an axial centrifugal compressor in dry (see Ref. [22]) and wet compression conditions.

With respect to the last work, some additional implementations were added: an improved data acquisition and control system, an additional plexiglass pipe for flow visualization at the compressor intake, and a new configuration of the inlet duct for the use of the water injection system (WIS).

This paper represents an important contribution to literature by describing the characteristics of a new robust test rig for the study of wet compression in stable and unstable conditions, and by presenting data which highlight the stability limit, together with the stall and surge behavior of the compressor tested, at different rotational speeds. In addition, this work highlights the potential and reliability of cyclostationary analysis (used by the authors of this paper for the first time in Ref. [23]), applied to miniaturized pressure transducers, for detecting stall and surge in both dry and wet conditions. This is an important result since it confirms that this new technique could be suitable for compressor stall and surge analysis.

Test Facility

The experimental facility is located at the Engineering Department Laboratory of the University of Ferrara. The test rig was exhaustively depicted in Refs. [22] and [23] but for this work, some significant implementations were performed in order to make the system suitable for water injection and to record data by a new hardware/software system.

The compressor tested, which is driven by an 87 kW asynchronous electric motor by means of a variable frequency drive, is the axial-centrifugal compressor of the Allison 250-C18 turboshaft engine. In this compressor, six axial stages are preceded by an inlet guide vane, and they are followed by a radial stage with a vaned diffuser. After the radial stage, the flow path continues with two semivolutes and respective circular conduits. The diameter of these outlet sections is 0.056 m whereas the intake diameter of the compressor is 0.104 m. The nominal characteristics of the compressor, and the range of operating conditions during tests, are reported in Table 1.

In this section, the main features of the test rig are presented and new implementations to the test bench are described in detail.

Compressor Piping System. The piping system was modified by changing the configuration of the inlet duct to allow water injection. In particular, the new configuration consists of an inlet duct which can be divided into three significant parts. The first part consists of a 1 m length 290 mm internal diameter plexiglass pipe, called "wet chamber," which contains four spray injectors—the water system will be described in the next subsection. This pipe is connected to a steel pipe (110 mm internal diameter and 1.5 m length) which precedes an orifice plate. The orifice plate is no longer installed as an edge orifice plate as in Ref. [22]; it has now two annular chambers for differential pressure measurement and is preceded by another steel pipe (110 mm internal diameter and 1.5 m length).

Table 1 Compressor operating characteristics

Nominal conditions	Rotational speed	51,600 rpm
	Mass flow rate	1.36 kg/s
	Pressure ratio	6.2
Operating conditions (dry) in the test rig	Rotational speed	8000–25,000 rpm
	Mass flow rate	0.15–0.57 kg/s
	Pressure ratio	1.02–1.78

At the compressor intake, a short plexiglass pipe was installed for flow visualization. This implementation was necessary in order to verify the presence and properties of water droplets reaching the compressor intake and to identify the type of flow pattern [24]. Figure 1 shows the short duct for flow visualization (Fig. 1(*b*)) and the overall inlet pipe described previously (Fig. 1(*a*)).

Downstream the compressor the flow path consists of a conveyor, an electric valve, valve 1, and an outlet duct which lead to a plenum of 1.5 m^3. Finally, the piping system ends with an outlet duct and another electric valve, valve 2.

The piping system is built so that two different layouts, layouts #1 and #2, can be obtained (see Fig. 3) depending on the type of tests to be carried out. Layout #1 is more suitable for steady-state map determination (even beyond the typical surge line, due to the small downstream volume) and stall analysis—in other words it is suitable for static instability analysis. On the other hand, layout #2 is most suitable for surge analysis (and stall evolution before surge)—in other words, it is suitable for dynamic instability analysis. Depending on the chosen configuration, valve 1 (in layout #1) or valve 2 (in layout #2) is used to regulate the mass flow rate.

Water Injection System. The WIS is connected to the department water system. When the WIS is turned on, the water passes through a demineralized water production system (DWPS), which consists of two vessels working in parallel and containing mixed bed exchange resins. The demineralized water is then accumulated in a tank (50 dm^3—sufficient to guarantee water injection for 1 h) which is directly connected to a volumetric pump and pressure control valve so that the demineralized water is pumped at about 50 bar toward the four injectors. Each of these injectors (hollow cone atomizer type) sprays demineralized water at a nominal pressure of 50 bar with a mass flow rate of 10.81 kg/h. A detailed description of these injectors and their characterization is summarized below. In Fig. 2, the DWPS and the injectors are shown with their respective manual valves. At the inlet section of each atomizer, there is a filter with 400 meshes, whereas the outlet section the injector has a cone shape for increasing the nebulizing effect on the water. Table 2 illustrates the main characteristics of the injectors used in this work.

Measurement Positions. In the test rig, both thermodynamic and vibroacoustic sensors are installed but this work focuses only on thermodynamic sensors (vibroacoustic equipment will not be discussed here). Figure 3 illustrates the thermodynamic sensors located along the circuit, i.e., pressure transducers, thermocouples and mass flow rate meters. The thermodynamic sensors used in this work are the same used in Ref. [22] (see Figs. 3 and 4). Thermocouples (J type and K type) were used, together with pressure transducers (membrane type) to study stable and unstable performance of the compressor. Moreover, two miniaturized fast respond transducers are positioned in the proximity of the compressor inlet since based on previous experimental analyses and theoretical reasoning, stall cells are undoubtedly generated at the first compressor stage.

This is due to the low compressor rotational speed during tests and the removal of the bleed valve [22,23].

The mass flow rate was measured by means of an orifice plate, at the compressor inlet, and by means of a hot wire sensor positioned downstream the plenum. Only one additional thermocouple was installed at the end of the plexiglass pipe for water injection (wet chamber) to measure the static temperature of the gas—the thermocouple was positioned so that water droplets could not reach it, determining significant errors due to evaporation phenomena.

Moreover, a tank in which the water is collected was positioned on a scale to determine the amount of residual water in the pipes. This operation was carried out by means of calibration of the injection system (see section *Methodology*) so as to estimate the

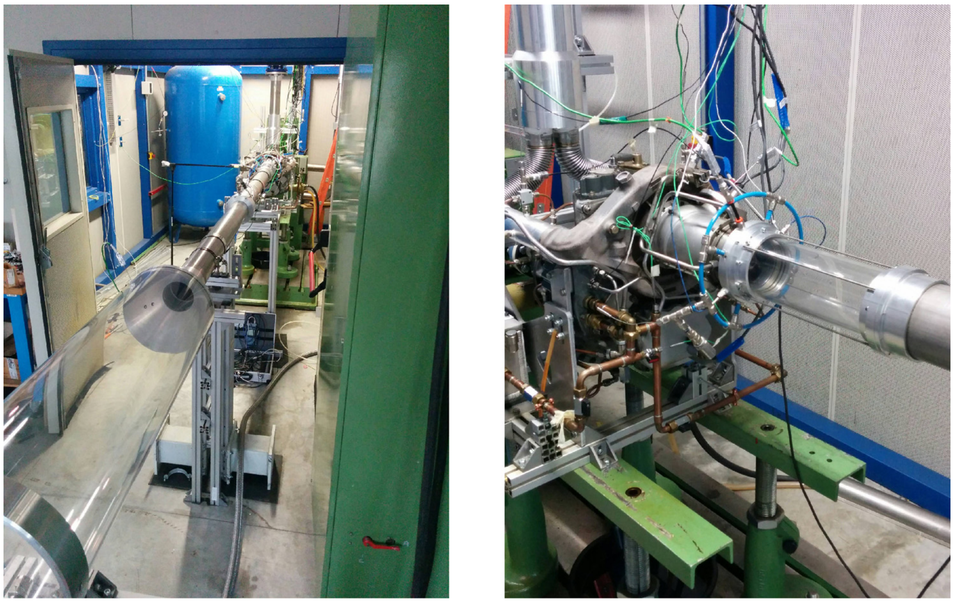

(*a*) (*b*)

Fig. 1 Inlet duct of the test rig: intake (*a*); compressor inlet (*b*)

water mass flow rate actually ingested by the compressor throughout the test, which is necessary to obtain the performance maps.

Control and Acquisition System. Measurement signals are acquired by a renewed data acquisition system. New hardware components were installed to substitute the previous configuration. In the past, two or more acquisition units were used and managed by the same homemade software developed in LabVIEW®, in order to acquire and collect high frequency and low frequency data in parallel. However, this configuration caused the increase in process load of the control PC and did not ensure accurate simultaneous acquisition of the data. This issue was solved in this work by integrating a NI cDaq 9188 XT (equipped with 8 slots) in replacement of NI cDaq 9174 and SCXI 1000 previously configured. This solution implied a reduction to the maximum number of sensors implemented but also significantly lower electric and electromagnetic noise, which can severely affect the results of accelerometers and Kulite transducers, thanks to the particular cabling strategy used. Table 3 shows the different acquisition modules used and the related signals acquired. Obviously, the new hardware configuration also implied a significant simplification to the developed control and acquisition software.

Methodology

The methodology used in this work is the same described in Ref. [23]; thus in this section, it is only briefly summarized. Transient and steady-state tests were carried out in layout #2 at different rotational speeds.

Steady-state tests were carried out by applying a step-by-step closure of the control valve; the steps were 10 deg, far from the

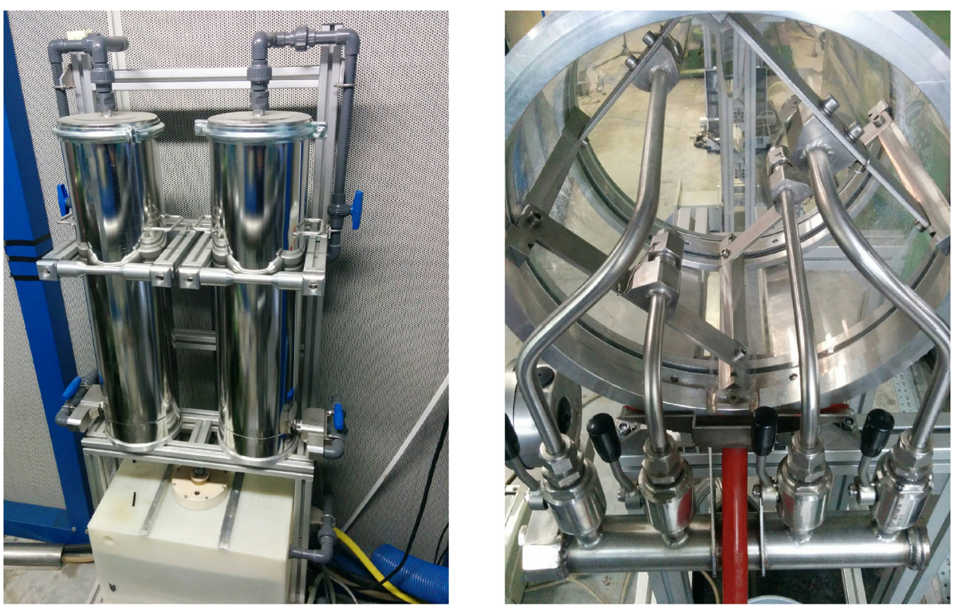

(*a*) (*b*)

Fig. 2 WIS: DWPS (*a*); hollow cone spray injectors and manual valves (*b*)

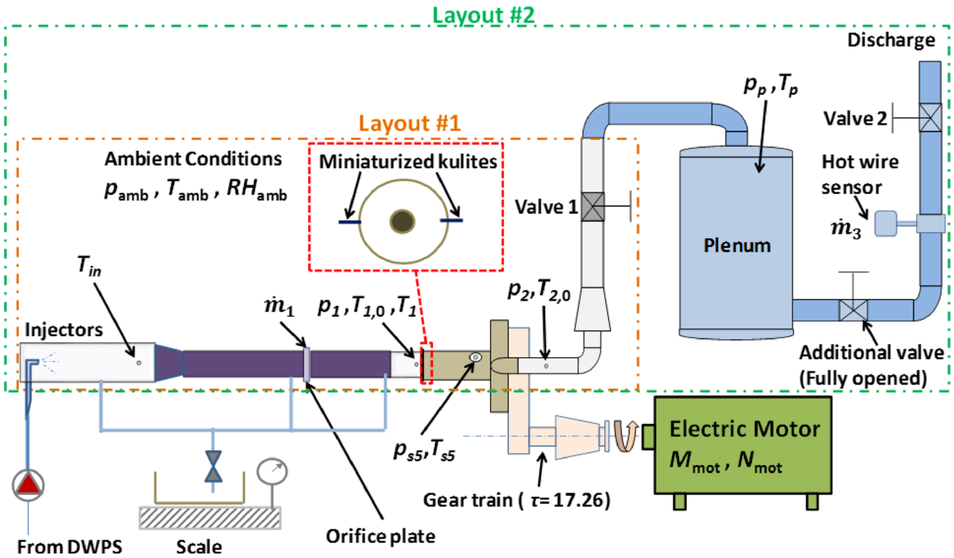

Fig. 3 Sketch of the test rig, layouts #1 and #2 (lateral view), with the installed measurement transducers

Table 2 Characteristics of a single injector

Type of flow out of the nozzle	Swirl jet - water takes a helical path
Type of spray	Spray cone—the spray angle is about 80 deg. The water is discharged with an axisymmetric cone shape
Materials	Elastomeric (main body); ceramic (nebulizing area)—this allows (i) compatibility with demineralized water, (ii) low weight, and (iii) long operating life
Installation	Threaded $^1/_4$ "NPT—this allows easy installation or replacement
Nominal operating pressure	50 bar—the pressure is regulated by a control valve downstream the volumetric pump. Injectors demonstrated optimum behavior starting from 7 bar—future works could involve different operating pressure
Mass flow rate at 50 bar	10.81 kg/s—Regulated by the volumetric pump. This mass flow rate could vary in the future
Droplets Sauter mean diameter (SMD)	16–34 μm (Manufacturer data)—The value can vary depending on the measurement method

surge line, and 5 deg in proximity to the expected instability onset. Data were acquired after waiting about 20–40 s for the stabilization of the compressor regime and signals.

Transient tests were carried out by imposing the continuous closing of the control valve until deep instability began. Due to the electric actuator characteristic, the valve closure rate was 1.5 deg/s. After the complete development of the instability phenomenon, the valve was dynamically reopened to restore stable conditions.

All the tests mentioned previously were conducted in dry conditions first and subsequently in wet conditions. Table 4 illustrates the tests carried out. Only the test results obtained in layout #2 are

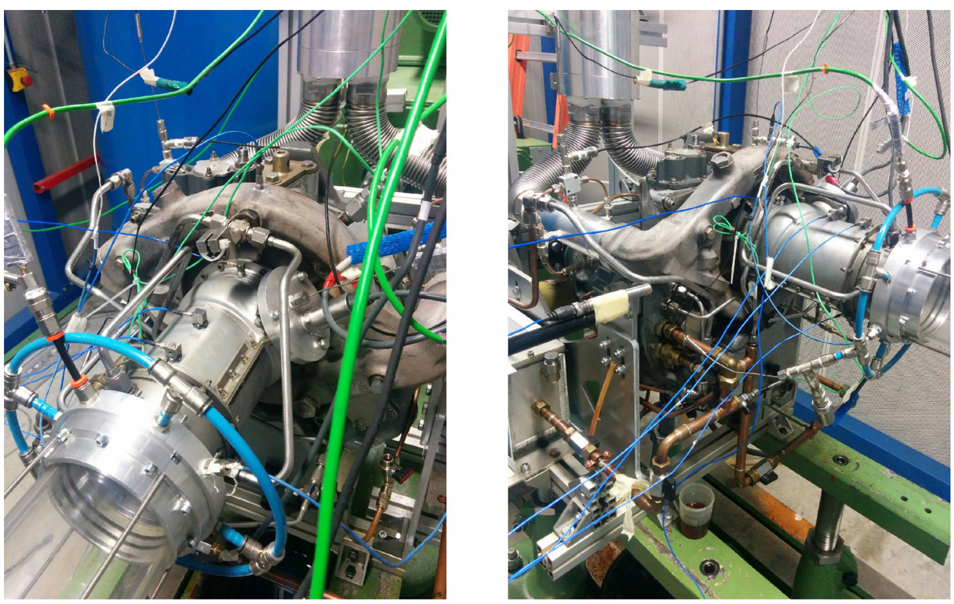

(*a*) (*b*)

Fig. 4 Instrumentation installed around the compressor

Table 3 Acquisition modules and sensors

Modules	C	Monitored sensors or controlled devices	Sampling frequency (Hz)
NI 9207	16 differential	Pressure sensors	50
NI 9213	32	Thermocouples	18
NI 9485	8	Inverter control	1000
NI 9269	4	Inverter and valve control	1000

presented in this paper, since that particular configuration of the test rig allows the identification of both rotating stall and deep surge.

The compressor performance in wet conditions was characterized by the evaluation of the actual mass flow of water injected. Therefore, before the experimental tests, the injection system was calibrated in order to find out the amount of water ingested by the compressor as a function of the air volume flow rate.

The calibration parameter used, which is also shown in the steady-state performance maps, is the water-to-air ratio (WAR)

$$\mathrm{WAR} = \frac{m_{\mathrm{wat,in},C}}{q_{\mathrm{in},C}} \quad (1)$$

This coefficient gives an indication of the ratio between the mass flow rate of water and the volumetric flow rate of air—it is a parameter analogous to gas volume fraction or liquid volume fraction. It is expressed in terms of $\mathrm{kg_{water}/m^3{}_{air}}$, but the same quantity can be expressed in terms of percentage concentration. The calibration procedure consisted of running the compressor at different velocities, and at each velocity, the water was injected for a certain amount of time (about 4 min)—the water ingested by the compressor was calculated as the water flow sprayed by the injectors, minus the drain water flow measured through the scale.

This calibration was performed only using two injectors and its results are shown in Fig. 5.

According to Refs. [21] and [25–27], the corrected nondimensional parameters are calculated as

$$N_C^* = \frac{N}{\sqrt{\gamma \cdot R \cdot T_1}} \cdot \frac{\sqrt{(\gamma \cdot R \cdot T_1)_{\mathrm{ref}}}}{N_{\mathrm{ref}}} \quad (2)$$

$$\mu_C^* = \frac{m_C \cdot \dfrac{\sqrt{T_1}}{p_1}}{\left(m_C \cdot \dfrac{\sqrt{T_1}}{p_1}\right)_{\mathrm{ref}}} \cdot \frac{\sqrt{\dfrac{R}{\gamma}}}{\sqrt{\left(\dfrac{R}{\gamma}\right)_{\mathrm{ref}}}} \quad (3)$$

where N_C* and μ_C* are the corrected rotational speed and corrected mass flow rate, respectively. The reference conditions are the ambient ISO conditions, $m_{\mathrm{ref}} = 0.42$ kg/s, and $N_{\mathrm{ref}} = 20{,}000$ rpm.

An attempt was also made to calculate the efficiency of the compressor when operating in wet compression. However, this estimation was hard to accomplish due to the water droplets which affect the measure of stagnation temperature. The values of efficiency found were not reasonable; future investigation will focus on a strategy to calculate isentropic efficiency in wet compression.

Accuracy. The evaluation of the uncertainty of results can be made based on preceding works carried out on the test rig with the same or comparable instrumentation to that presented in this paper. In dry conditions, the uncertainty analysis of the old version of the test rig (different system layout, limited acquisition and data analysis, and older sensors) was investigated in Ref. [28], and quite a large uncertainty of corrected mass flow rate and a lower value for compressor corrected rotational speed were found. However, these values only referred to the preliminary tests performed at that time.

Today, the test methodology is certainly improved, more accurate and advanced instrumentation is used, and many components and important measurement sections were designed in order to minimize the measurement errors.

Therefore, the results of Ref. [28] can only represent an upper limit for the current uncertainty of this new test rig data. The uncertainty of the corrected mass flow rate in this work is ±1.9%.

In wet compression conditions, measurements are more critical since they can be affected by the presence of water droplets; therefore, some assumptions are necessary, and piping system design has to be considered, when evaluating compressor performance. Due to the length of the inlet duct, evaporation and sensible heat exchange between air and water cannot be neglected, likewise for humidity.

Table 4 Experiments carried out and ambient conditions during tests in layout #2

Corrected rotational speed		Type of test	p_{amb} (mbar)	RH_{amb} (%)	T_{amb} (°C)
Dry	0.4	Steady-state	1006	31.3	21.1
		Transient	1006	31.2	21.1
Wet	0.4	Steady-state	1007	31.8	20.6
		Transient	1007	31.8	20.7
Dry	0.5	Steady-state	1004	30.0	21.3
		Transient	1004	30.3	21.3
Wet	0.5	Steady-state	1003	29.8	22.1
		Transient	1003	29.8	21.2
Dry	0.9	Steady-state	1004	30.1	20.6
		Transient	1004	30.1	20.6
Wet	0.9	Steady-state	1003	29.8	21.2
		Transient	1002	34.0	20.5
Dry	1.01	Steady-state	1006	31.2	21.2
		Transient	1006	31.3	21.1
Wet	1.01	Steady-state	1006	32.9	20.8
		Transient	1006	32.9	20.8
Dry	1.25	Steady-state	1003	30.6	21.0
		Transient	1003	30.6	21.1
Wet	1.25	Steady-state	996	32.2	19.5
		Transient	996	32.3	19.4

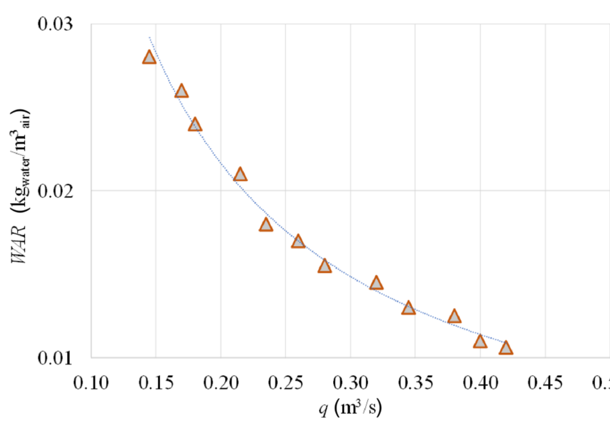

Fig. 5 Injection system calibration

For this reason, the air at the compressor inlet is assumed to be very humid (not necessarily fully saturated). In addition, experimental observation of the flow pattern revealed the presence of small droplets within the flow and coagulated droplets flowing along the internal surface of the pipe. Thus, since the stagnation temperature is significantly affected by the presence of water this measure is not reliable during tests.

Also, static temperature is measured by means of an annular ring to prevent the deposition of residual nonevaporated water droplets. Regarding temperature measurements at the compressor discharge, the air may be fully saturated or oversaturated; in the first case, the stagnation temperature measurement is reliable, whereas in the second case it is not. Thus, as for the inlet stagnation temperature, the recorded values of outlet stagnation temperature cannot be considered reliable.

To prevent any potential error in thermodynamic performance analyses, in this work the static pressure ratio is used. It is important to highlight that the assumptions made for the determination of performance maps of the compressor in wet conditions are approximately 2.5% for the rotational speed, and 2.5% for the mass flow rate (measured with a hotwire sensor positioned downstream the plenum, which acts as a phase separator).

Based on literature results [24], the error of the orifice plate in calculating the gas volume flow rate when metering a wet gas flow is in the range of 2.5% as well. This is due to the fact that such a low amount of water can generate an under-reading within 2.5% but there is currently no correlation to correct this type of measurement shift.

Results and Discussion

As shown in Table 4, many tests were carried out and in this section all the results are presented. In particular, thermodynamic analysis in steady-state and transient conditions was performed by processing the experimental data obtained in layout #2.

The orifice plate results were shown to be consistent with the hot wire sensor results in dry and wet conditions as well, although a there was a slight under-reading within 1%. This reflects what was found in literature for wet gas metering with low liquid content [24]. De facto, the measurement shift was noticed during a calibration of the orifice plate data by comparing the results with the hot-wire sensor response (data alignment using the hot wire sensor as a sample device). Therefore, the results of the mass flow rate at the compressor upstream and plenum downstream recorded throughout steady-state and dynamic tests in wet and dry conditions can be considered consistent with each other.

Steady-State Tests (Performance Analysis). Steady-state tests were carried out in layout #2 at the following approximate actual rotational speeds: 8000, 10,000, 18,000, 20,000 and 25,000 rpm. Experiments were conducted in dry and wet conditions setting the corrected rotational speed around these speeds.

Figures 6 and 7 illustrate, respectively, the overall characteristic curve and the required driving torque to operate the compressor at the rotational speeds tested. The data are reported for both dry and wet conditions.

As can be seen, WAR is in the range 0.9–3.3% using two injectors during experiments (obviously these values represent estimations based on calibration data, Fig. 5). The performance curves are evaluated by means of the static-to-static pressure ratio, β, since stagnation measurements cannot be correctly calculated due to the presence of water (this is comprehensively explained in Ref. [21]). It can be noted from Fig. 6 that the injection of water led to an increase in β, at each rotational speed tested, but this increase was more evident at higher rotational speeds ($N_C{*} = 0.90$, $N_C{*} = 1.01$ and $N_C{*} = 1.25$). However, Fig. 7 shows that this phenomenon is accompanied by the increase in torque,—in this case the increase is more significant at higher rotational speeds, $N_C{*} = 1.01$ and $N_C{*} = 1.25$)—which potentially means an increase in power consumption for running the compressor.

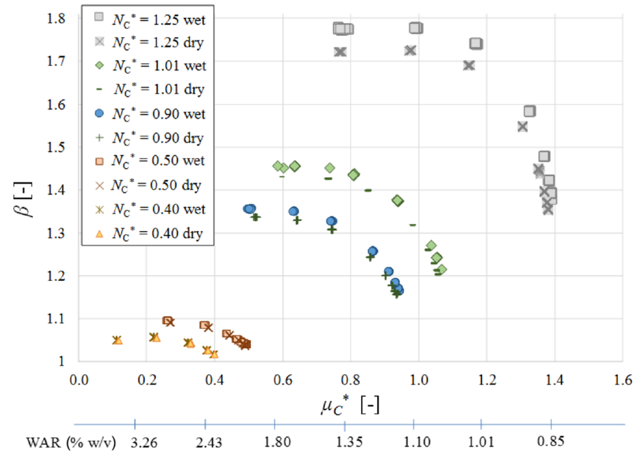

Fig. 6 Steady-state compressor map: static-to-static pressure ratio

Steady-state tests revealed that in wet compression conditions surge occurred with a very similar closing angle value, compared to dry conditions. The flow rate values in the curves of Figs. 6 and 7 represent average values. Since near surge the mass flow rate is more susceptible to variations in both dry and wet conditions, it is difficult to accurately note an extension or reduction in the operating range of the compressor near surge at each speed tested.

It is a speculation that wet conditions generate a slight extension of the operating range but further investigations are required by testing the compressor at different WAR values.

Transient Behavior. These types of tests were carried out to detect stall and surge from the measurement data—also in this section a comparison between dry and wet conditions is presented.

The response of the thermodynamic sensors was collected throughout all the tests while valve 2 was dynamically closed from fully open until surge occurred. This allowed both surge characteristics and rotating stall evolution, and the difference between dry and wet tests, to be identified as shown in the next subsections.

Surge Analysis. This subsection presents data at $N_C{*} = 0.90$ but analogous behavior was also found at the other tested rotational speeds. The valve closure was stopped at surge onset to let instability develop for a certain amount of time (for instability characterization).

Figures 8 and 9 show the main recorded thermodynamic quantities throughout the tests in dry and wet conditions, respectively.

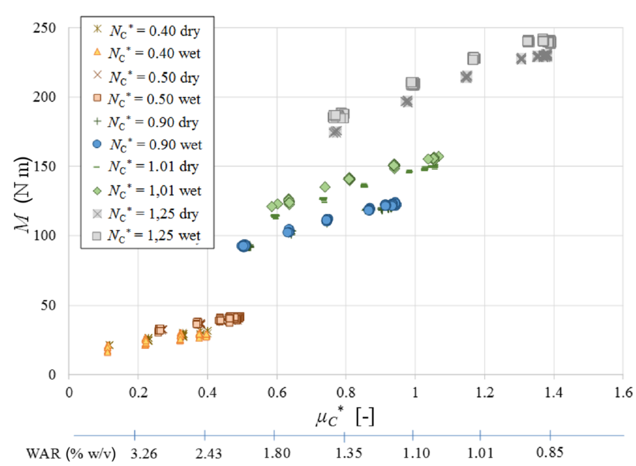

Fig. 7 Steady-state results: required driving torque

By looking at the pressure and mass flow rate trends of Fig. 8, surge can be clearly identified by the strong fluctuations of data (p_1, p_2, m_1, m_3) due to surge pulsations. Deep surge began at $\alpha = 31\%$ but the compressor recovered from instability at $\alpha = 39\%$ when the valve was reopened. This confirms the hysteresis phenomenon found in Ref. [22]. An important thing to note is that m_3 presented low amplitude oscillations (with respect to m_1) during surge; this was due to the damping effect of the plenum on its downstream pipe.

The same test was carried out in wet conditions and the results are presented in Fig. 9 (with two water injectors activated). It appears clear that surge occurred at a percentage closing angle $\alpha = 30\%$, thus valve closure was stopped.

It can be seen that, as previously mentioned, the mass flow rate measured by the orifice plate was not significantly influenced by the effect of water injection. Some differences between m_1 and m_3, are evident throughout the dynamic closure and reopening of the valve—this is due to different transient phenomena occurring at compressor upstream and plenum downstream during the mass flow reduction. For this reason, the orifice plate provided different results from the hot-wire sensor (which is not affected by the presence of water due to its location in the test rig).

A last important aspect to underline by comparing Figs. 8 and 9 is the smaller hysteresis effect (although the difference is not significant) which can be noted in wet compression. With water injection, surge occurred at $\alpha = 30\%$ and was recovered only at $\alpha = 36\%$ compared to dry conditions. This could be relevant in terms of potential damage to the compressor and its components and might indicates that "wet surge" seems to be as recoverable as "dry surge," if a low amount of water is injected.

However, to better analyze the effect of wet compression on pressure fluctuation during surge the data presented in Figs. 8 and 9 were compared.

Figure 10 illustrates a comparison between pressure oscillations in dry surge and wet surge. Surge pulsations in terms of outlet pressure, p_2, are comparable but slightly increased from dry ($\Delta p_{2,\max,dry} \sim 0.13$ bar) to wet conditions ($\Delta p_{2,\max,wet} \sim 0.14$ bar). Similar considerations can be made for p_1, as shown in Fig. 10. The action of the water injection also caused a slight positive shift in the p_2 and p_1 values of about 0.02 bar from dry to wet, and the decrease in surge frequency (from ~0.43 to ~0.41 Hz) as shown in Fig. 10.

The differences from wet surge and dry surge which have been revealed in this section might sound irrelevant but considering the very low amount of water, it might imply that higher quantities of water further increase the severity of wet surge [29–31] and also the compressor piping system behavior in case of emergency shutdown events [32].

Rotating Stall Analysis. Rotating stall was studied by means of two piezoresistive pressure transducers (kulites) since their position allows the observation of stall cells at the first stage of the compressor.

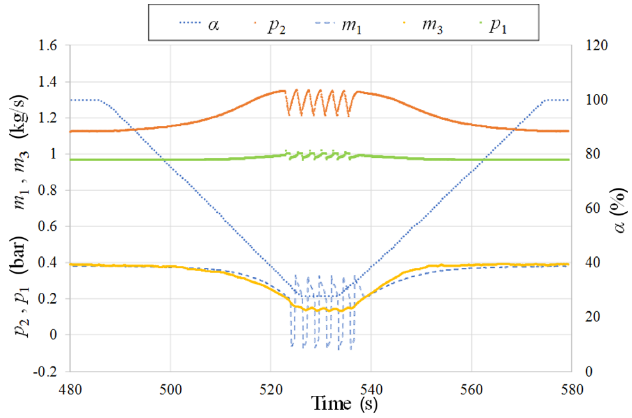

Fig. 9 Dynamic test at $N_c^* = 0.9$: thermodynamic data time series—wet conditions

Since stall and surge were proven to be cyclostationary phenomena, as also demonstrated in Ref. [23], a cyclostationary analysis has been carried out on the kulite signals (Figs. 11 and 12).

Figure 11 shows the results of one kulite (the other one showed very similar results), in dry and wet conditions at $N_c^* = 0.90$, through two waterfall diagrams that report the sensor response throughout the transient test (dynamic closure of valve 2). The waterfall diagrams were obtained by means of cyclostationary analysis [23] which allows the cyclic frequencies λ, which modulate the signal, to be identified as a function of the percentage closing angle (in the case of a wall pressure transducer, a modulation can be caused by a rotating stall cell). The figure also shows the corresponding operating point of the compressor so as to correlate the surge onset to flow as well as valve positions.

The waterfall of Fig. 11(*a*) shows that, from the beginning of the test, a rotating stall cell rotates at about $\lambda = 18$ Hz. The fact that this rotating stall cell is present even with the valve completely open was comprehensively explained in Refs. [22] and [23] and is due to the low rotational speed combined with the removal of the bleed valve from the compressor. This cell has a harmonic component, which may represent a second stall cell at the same stage; however, without additional sensors it is difficult to demonstrate this—therefore, this paper only refers to one cell.

The rotating stall cell begins to move in frequency while the valve is closing, in particular the frequency increases toward surge. In transient conditions, this does not necessarily mean that the cell is increasing its speed. This effect could be due to the increase in size of the cell. This phenomenon continued until

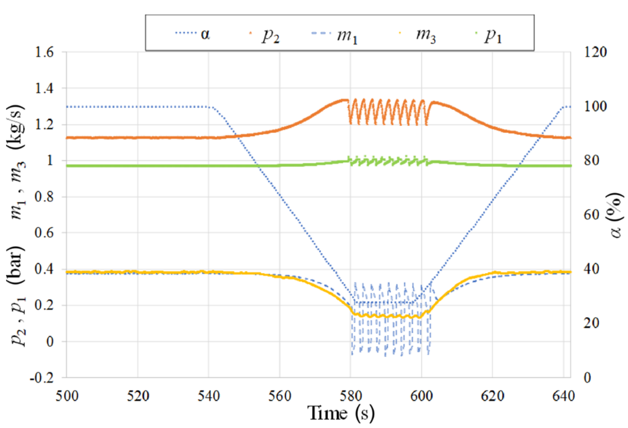

Fig. 8 Dynamic test at $N_c^* = 0.9$: thermodynamic data time series—dry conditions

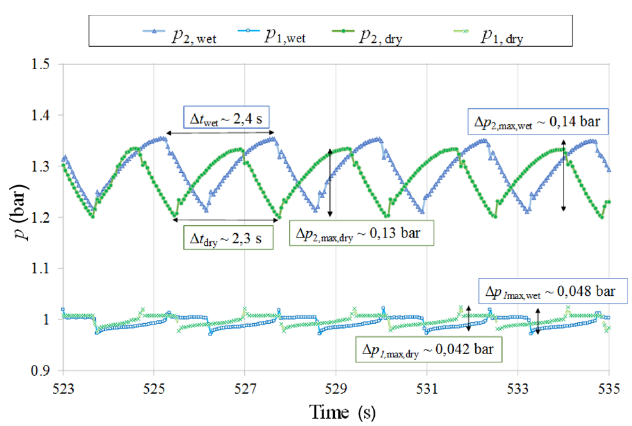

Fig. 10 Dynamic test at $N_c^* = 0.9$: comparison of pressure fluctuation during surge in dry and wet conditions

ID: asme3b2server Time: 22:45 I Path: //chenas03.cadmus.com/Cenpro/ApplicationFiles/Journals/ASME/GTP#/Vol00000/190006/Comp/APPFile/AS-GTP#190006

surge occurred, which is visible by the low cyclic frequency component (surge frequency) which arises. As seen in preceding experiments [22,23], during surge, stall cell cyclic frequency is still present although with reduced amplitude and scattered frequency value. This again confirms that at low rotational speeds, the instability of this compressor is characterized by both stall and surge which alternatively takes place during the surge process.

Figure 11(*b*) shows the same tests in wet compression. Although the rotating stall cell seems to behave analogously to the dry conditions, there is a slight increase in perturbation

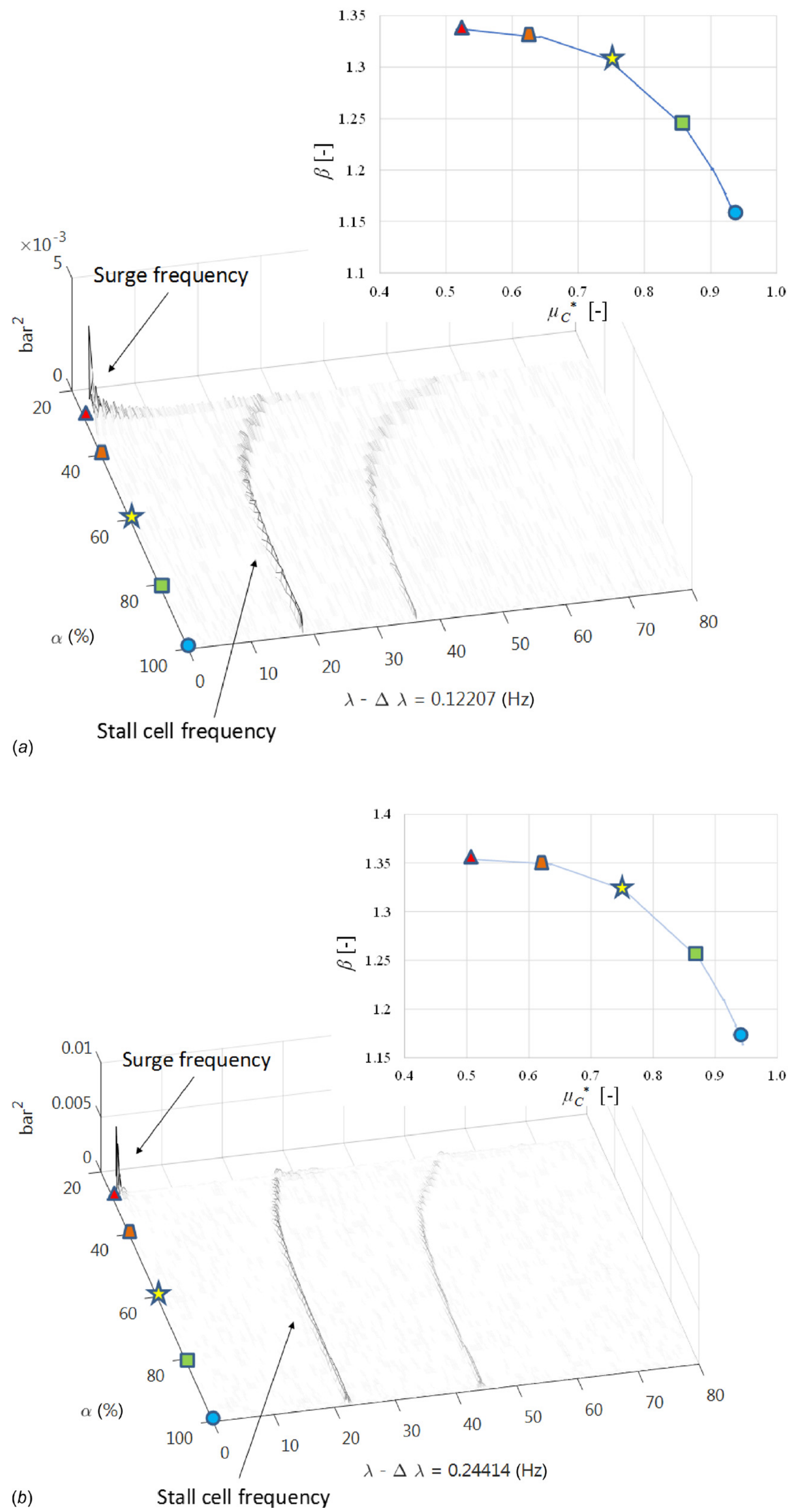

Fig. 11 Dynamic test at $N_c^* = 0.90$—cyclostationary analysis, rotating stall cell: dry conditions (*a*); wet conditions (*b*)

amplitude (even if this is not apparent in the figure). Moreover, a clear shift in frequency is shown, compared to the dry test (Fig. 11(*a*)). In the case of wet compression (stall cells may be called "*wet stall cells*"), the wet stall cell modulation frequency is about $\lambda = 24$ Hz, which means that water injection affects the rotating stall cell characteristics. Also, the change in frequency while the valve is closing seems to have different features; in particular, in wet compression this change appeared less significant.

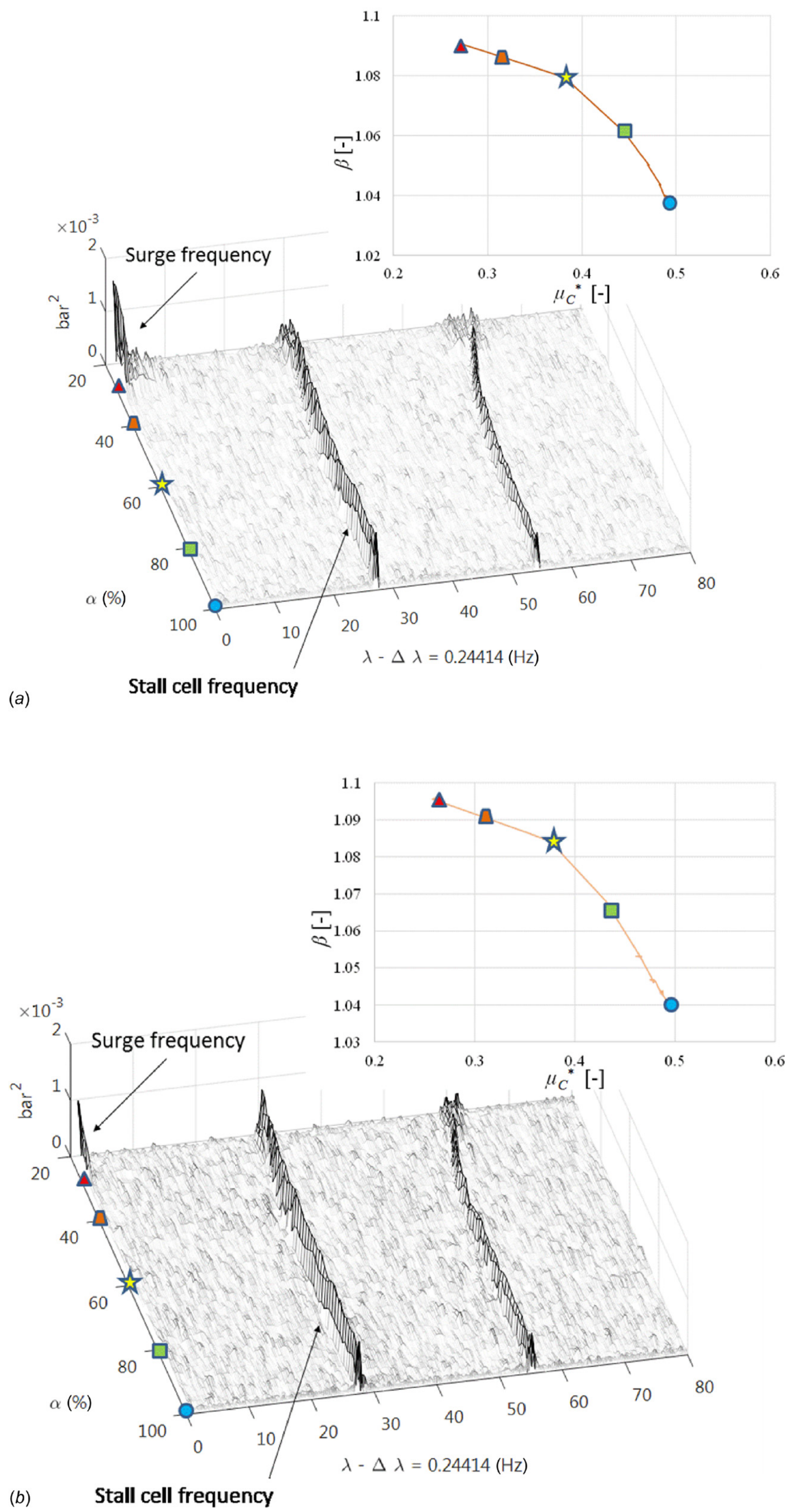

Fig. 12 Dynamic test at $N_c^* = 0.50$—cyclostationary analysis, rotating stall cell: dry conditions (*a*); wet conditions (*b*)

This can be explained by the water droplets ingested by the compressor which probably affect the formation, velocity, and increase in rotating stall cells.

This is a speculation based on the results and cannot be confirmed with high certainty since literature on this topic is insufficient. In order to give relevance to this theory, the same comparison between wet and dry conditions with an analogous test (transient test—layout #2) was carried out at a lower rotational speed ($N_c^* = 0.50$), at which the compressor actually ingested less water. This comparison is shown in Fig. 12.

In this case, the cyclic frequency of the stall cell in dry conditions is $\lambda = 27$ Hz (Fig. 12(*a*)) whereas in wet conditions it is $\lambda = 28$ Hz (Fig. 12(*b*)). Moreover, at this rotational speed ($N_c^* = 0.50$), the change in the stall cell cyclic frequency during the closure of the valve in wet conditions is very similar to that observed in dry tests. The results seem to confirm the theory that water droplets affect the stall cell features and thus the stall cell internal flow characteristics, resulting in different stall cell speeds and/or sizes and affecting the formation process.

Based on these results, the more water ingested by the compressor, the more different the stall cell characteristics are.

Obviously, this phenomenon is probably more evident at the first compressor stage, where water has not evaporated and droplets are (almost) always present and cause strong impacts on the blades and thus on rotating stall cells.

More instrumentation is needed to investigate this topic in detail, but this paper undoubtedly offers important preliminary considerations and results.

AQ7 A significant aspect to highlight is that the typical FFT analysis, applied to the two kulites, showed consistent results to those obtained with cyclostationary analysis. This fact can be verified by comparing the results of Figs. 12 and 13; carrier frequencies f identified by FFT analysis reflect cyclic frequencies identified by cyclostationary analysis. From this derives the fact that cyclostationary analysis is effectively a powerful instrument for stall and surge analysis.

Limitations

The limitations of this study are closely related to the instrumentation used and thus to the impossibility of measuring important thermodynamic quantities, useful to achieve a better characterization of compressor performance in wet compression. The two most important limitations are listed below.

Measurement of the Stagnation Temperature. This represents the most important limitation since without knowing this quantity, the calculation of the isentropic efficiency, and total-to-total pressure ratio is not possible. The outlet stagnation temperature can be correctly measured only if the water completely evaporates throughout the compressor, or if the flow pattern is such that the hot junction of thermocouples is not wet by droplets. Other two linked parameters are the droplet evaporation along the compressor and the humidity at the compressor outlet. These parameters would be complementary relevant information.

Droplet Characterization at the Compressor Inlet and Outlet. The characterization of the droplet size at the injectors outlet was carried out in Ref. [21] by means of a laser Doppler anemometer. Unfortunately, that characterization is not useful in this work due to the length of the inlet duct and to the presence of the orifice plate. Therefore, it is difficult to predict what phenomena actually occur at the compressor intake and how exactly water droplets can affect wet stall cells. As mentioned in the section *Compressor piping system*, a new short plexiglass pipe was installed at the compressor intake, so as to allow a detailed droplet characterization in future works—the same strategy will be applied to the compressor outlet section.

Another important limitation is the methodology used for calibrating the injection system and thus determines the exact amount of water ingested by the compressor throughout tests, especially dynamic tests.

Moreover, only a small amount of water was sprayed (approximately WAR < 3%), so a careful sensitivity analysis on the compressor performance with a higher level of water cannot be achieved.

Conclusions

This paper presents an experimental analysis to evaluate the performance of an axial centrifugal compressor installed at the Engineering Department of the University of Ferrara.

The study focuses on both steady-state tests, for evaluating both compressor maps and the required driving torque, and transient tests, to analyze stall and surge phenomena.

Data obtained in wet compression conditions were compared with those in dry conditions to highlight the effect of water injection on compressor performance (stable and unstable regime). Steady-state tests revealed an increase in the static-to-static pressure ratio due to water injection—this phenomenon is more evident at higher rotational speeds, at which the amount of water ingested by the compressor increased. This fact is accompanied by a slight increase in the driving torque required by the compressor, which implies an increase in power consumption compared to dry conditions—this phenomenon was more evident at higher speeds as well. This agrees with many published works and also confirms the mentioned phenomenon for the tested axial-centrifugal compressor. From data observations, it appears that wet conditions generate a slight extension of the operating range but further investigations are required with a higher quantity of water.

Transient tests were carried out to determine the effect of injected water droplets on rotating stall and surge. Analysis of surge data showed that:

- Wet compression allows a very small delay in surge onset. Essentially, in wet conditions a slightly greater closure of the control valve ($\alpha = 30\%$) was necessary to cause surge onset, compared to dry conditions ($\alpha = 31\%$).
- The combined action of water injection and lower α caused a slight reduction in surge frequency from dry (~0.43 Hz) to wet conditions (~0.41 Hz) and an increase in discharge and suction pressure oscillation amplitudes.
- Wet surge caused a similar hysteresis effect (the compressor recovered from surge with about the same delay observed in dry conditions). This may be valid only for low quantities of water ingested. If a higher amount of water is injected, the results may change significantly.

In addition, by means of two miniaturized pressure transducers located at the first compressor stage, an analysis of rotating stall in wet compression was also carried out, which is relevant because, to the knowledge of the authors, literature does not offer many works on this topic.

Analysis of data on rotating stall showed that stall cells are influenced by the presence of water. In particular, their formation process, velocity, and growth are affected by water droplets. The more water ingested by the compressor, the more the rotating stall features change from dry to wet conditions.

At $N_c^* = 0.50$, the stall cell frequency was only slightly higher in wet conditions, compared to dry conditions, whereas when the compressor rotational speed, and thus the ingested water, was increased, the difference in terms of frequency and change of frequency throughout the valve closure was more evident. The signal of the two miniaturized transducers was analyzed by means of cyclostationary analysis, and the results were confirmed by means of a typical FFT analysis applied to these sensors. This testifies that stall and surge can be seen as cyclostationary phenomena, which is a significant conclusion that supports previous investigations of the authors of the paper.

This paper presented significant data on stall and surge in wet compression, which is not easy to find in literature. Future activity

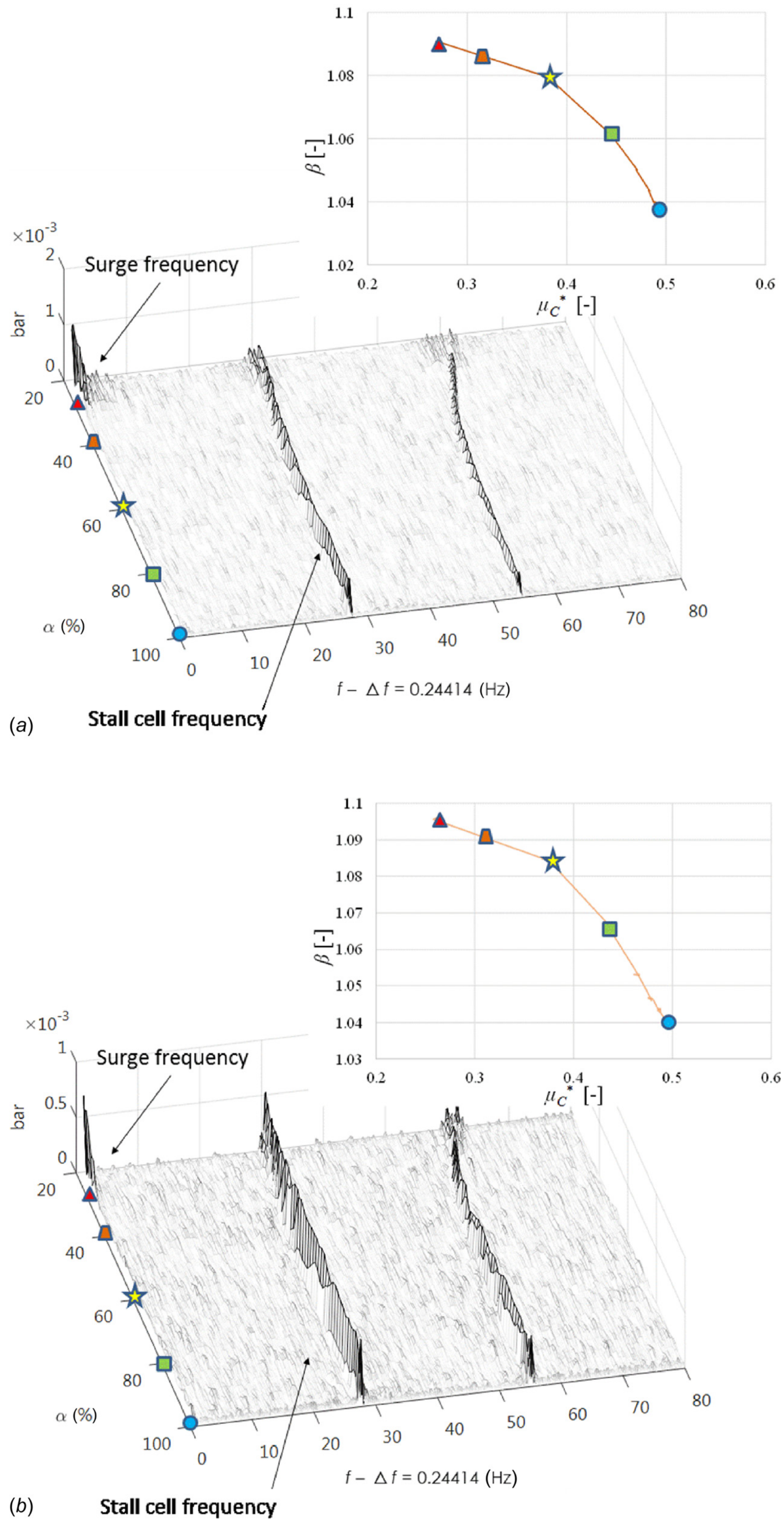

Fig. 13 Dynamic test at $N_c^* = 0.50$—FFT analysis, rotating stall cell: dry conditions (*a*); wet conditions (*b*)

will also be the analysis of the vibroacoustic data so as to make a comparison with thermodynamic results, in dry and wet conditions.

Nomenclature

c = number of acquisition channels
f = frequency
L = effective length
m = mass flow rate
M = torque
N = rotational speed
N^* = corrected rotational speed
p = pressure

ID: asme3b2server Time: 22:45 I Path: //chenas03.cadmus.com/Cenpro/ApplicationFiles/Journals/ASME/GTP#/Vol00000/190006/Comp/APPFile/AS-GTP#190006

q = volumetric flow rate
R = gas constant
RH = relative humidity
T = temperature
WAR = water-to-air ratio
α = throttling valve position percentage
β = pressure ratio
γ = ratio of the specific heats
Δp = pressure variation
Δt = time variation
λ = cyclic frequency
μ^* = corrected mass flow rate
τ = gear ratio

Subscript and Superscript

amb = ambient conditions
C = compressor
cDAQ = NI Compact DAQ
dry = dry conditions
el = electric quantity
in = inlet
mot = electric motor
max = maximum
min = minimum
p = plenum
ref = reference conditions
s5 = section at fifth axial stage
wat = water
wet = wet compression condition
0 = stagnation physical quantity
1,2,3 = test rig sections and segments

References

[1] Vigdal, L. A. B., and Bakken, L. E., 2017, "Variable Inlet Guide Vane Losses and Their Effect on Downstream Impeller and Diffuser in Wet Gas Flow," ASME Paper No. GT2017-64783.

[2] Poerner, M., Cater, R., Nolen, C., Musgrove, G., and Ransom, D., 2017, "Wet Gas Compression: Characterizing Two-Phase Flow Inside a Compressor With Flow Visualization," ASME Paper No. GT2017-64541.

[3] Mæland, D., and Bakken, L. E., 2017, "Wet Gas Compression: Test Conditions and Similitude," ASME Paper No. GT2017-64374.

[4] Brun, K., Gonzales, L. E., and Platt, J. P., 2008, "Impact of Continuous Inlet Fogging and Overspray Operation on GE 5002 Gas Turbine Life and Performance," ASME Paper No. GT2008-50207.

[5] Bhargava, R. K., Meher-Homji, C. B., Chaker, M. A., Bianchi, M., Melino, F., Peretto, A., and Ingistov, S., 2007, "Gas Turbine Fogging Technology: A Stateof-the-Art Review—Part I: Inlet Evaporative Fogging—Analytical and Experimental Aspects," ASME J. Eng. Gas Turbines Power, **129**(2), pp. 443–453.

AQ8 [6] Jolly, S., and Cloyd, S., 2003, "Performance Enhancement of GT24 With Wet Compression," Power-Gen International, Las Vegas, NV, ■, ~~pp. 9–11.~~

AQ9 [7] Ingistov, S., 2002, "Interstage Injection Into Axial Compressor, Gas Turbine Model 7EA," ASME Paper No. GT 2002-30656.

[8] Bianchi, M., Branchini, L., De Pascale, A., Melino, F., and Peretto, A., 2007, "NOX Reduction by Means of the Inlet Fogging Approach," ECOS 20th International Conference on Efficiency, Cost, Optimization, Simulation and Environmental Impact of Energy Systems, Padova, Italy, ■, ~~pp. 25–28.~~

[9] Schick, R. J., and Knasiak, K. F., 2000, "Spray Characterization for Wet Compression Gas Cooling Applications," Eighth International Conference on Liquid Atomization and Spray Systems, Pasadena, CA, ■, ~~pp. 16–20.~~

[10] Carraretto, C., 2006, "Power Plant Operation and Management in a Deregulated Market.," Energy, **31**(6–7), pp. 1000–1016.

[11] Brun, K., Kurz, R., and Simmons, H., 2006, "Aerodynamic Instability and Life-Limiting Effects of Inlet and Interstage Water Injection Into Gas Turbines," ASME J. Eng. Gas Turbines Power, **128**(3), pp. 617–625.

[12] ~~Li, M., and Zheng, Q., 2004, "Wet Compression System Stability Analysis Part I—Wet Compression Moore Greitzer Transient Model," ASME Paper No. GT2004-54018.~~

[13] Bhargava, R. K., Bianchi, M., Melino, F., Peretto, A., and Spina, P. R., 2008, "Influence of Compressor Performance Maps Shape on Wet Compression," ASME Paper No. GT2008-50761.

[14] Morini, M., Pinelli, M., Spina, P. R., and Venturini, M., 2010, "Influence of Blade Deterioration on Compressor and Turbine Performance," ASME J. Eng. Gas Turbines Power, **132**(3), p. 032401.

[15] Day, I., Williams, J., and Freeman, C., 2008, "Rain Ingestion in Axial Flow Compressors at Part Speed," ASME J. Turbomach., **130**(1), p. 011024.

[16] Roumeliotis, I., and Mathioudakis, K., 2007, "Water Injection Effects on Compressor Stage Operation," ASME J. Eng. Gas Turbines Power, **129**(3), pp. 778–784.

[17] Minghong, L., and Qun, Z., 2004, "Wet Compression System Stability Analysis—Part I," ASME Paper No. GT2004–54018.

[18] Qun, Z., and Minghong, L., 2004, "Wet Compression System Stability Analysis—Part II," ASME Paper No. pp. GT2004–54020.

[19] Gröner, T. G., and Bakken, L. E., 2012, "Instability Characteristic of a Single-Stage Centrifugal Compressor Exposed to Dry and Wet Gas," ASME Paper No. GT2012–69473.

[20] Ferrara, V., and Bakken, L. E., 2015, "Wet Gas Compressor Surge Stability," ASME Paper No. GT2015-42650.

[21] Bettocchi, R., Morini, M., Pinelli, M., Spina, P. R., Venturini, M., and Torsello, G., 2011, "Setup of an Experimental Facility for the Investigation of Wet Compression on a Multistage Compressor," ASME J. Eng. Gas Turbines Power, **133**(10), p. 102001.

[22] Munari, E., Morini, M., Pinelli, M., Spina, P. R., and Suman, A., 2017, "Experimental Investigation of Stall and Surge in a Multistage Compressor," ASME J. Eng. Gas Turbines Power, **139**(2), p. 022605.

[23] Munari, E., D'Elia, G., Morini, M., Mucchi, E., Pinelli, M., and Spina, P. R., 2018, "Experimental Investigation of Vibrational and Acoustic Phenomena for Detecting the Stall and Surge of a Multistage Compressor," ASME J. Eng. Gas Turbines Power, **140**(9), p. 092605.

[24] Munari, E., Pinelli, M., and Spina, P. R., 2018, "Wet Gas Flow rate measurements by Means of Single Phase Meters," ASME Paper No. GT2018-76190.

[25] AGARD, 1995, "Recommended Practices for the Assessment of the Effects of Atmospheric Water Injection on the Performance and Operability of Gas Turbines Engines," Research and Technology Organization, Neuilly-sur-Seine, France, Report No. AGARD-AR-332.

[26] Mathioudakis, K., and Tsalavoutas, A., 2002, "Uncertainty Reduction in Gas Turbine Performance Diagnostic by Accounting for Humidity Effects," ASME J. Eng. Gas Turbines Power, **124**(4), pp. 801–808.

[27] Roumeliotis, I., and Mathioudakis, K., 2010, "Evaluation of Water Injection on Compressor and Engine Performance and Operability," Appl. Energy, **87**(4), pp. 1207–1216.

[28] Bettocchi, R., Pinelli, M., and Spina, P. R., 2005, "A Multistage Compressor Test Facility: Uncertainty Analysis and Preliminary Test Results," ASME J. Eng. Gas Turbines Power, **127**(1), pp. 170–177.

[29] Brun, K., Simons, S., Kurz, R., Munari, E., Morini, M., and Pinelli, M., 2018, "Measurement and Prediction of Centrifugal Compressor Axial Forces During Surge—Part I: Surge Force Measurements," ASME J. Eng. Gas Turbines Power, **140**(1), p. 012601.

[30] Munari, E., Morini, M., Pinelli, M., Brun, K., Simons, S., and Kurz, R., 2018, "Measurement and Prediction of Centrifugal Compressor Axial Forces During Surge—Part II: Dynamic Surge Model," ASME J. Eng. Gas Turbines Power, **140**(1), p. 012602.

[31] Munari, E., Morini, M., Pinelli, M., Brun, K., Simons, S., and Kurz, R., 2019, "A New Index to Evaluate the Potential Damage of a Surge Event: The Surge Severity Coefficient," ASME J. Eng. Gas Turbines Power, **141**(3), p. 031017.

[32] Munari, E., Morini, M., Pinelli, M., Brun, K., Simons, S., Kurz, R., and Moore, J., "An Advanced Surge Dynamic Model for Simulating ESD Events and Comparing Different Anti-Surge Strategies," ASME J. Eng. Gas Turbines Power, **141**(7), p. 071003.